Morphology-induced magnetic phase transitions in Fe deposits on MgO films investigated with XMCD and STM

P. Torelli,[1] S. Benedetti,[1] P. Luches,[1] L. Gragnaniello,[1,2] J. Fujii,[3] and S. Valeri[1,2]
[1]*INFM-CNR, National Research Centre for NanoStructures and BioSystems at Surfaces (S3), Via Campi 213/A, 41100 Modena, Italy*
[2]*Dipartimento di Fisica dell'Università di Modena e Reggio Emilia, Via Campi 213/A, 41100 Modena, Italy*
[3]*TASC Laboratory, INFM-CNR, Area Science Park, S.S. 14, Km. 163.5, I-34012 Trieste, Italy*
(Received 20 March 2008; revised manuscript received 26 November 2008; published 13 January 2009)

The interplay between magnetic properties and morphology of thin iron deposits on MgO films grown on Ag(001) was investigated by means of x-ray magnetic circular dichroism and scanning tunneling microscopy (STM) measurements as a function of the Fe thickness and after postgrowth thermal treatments. The as-grown Fe deposits display a sharp transition as a function of the Fe thickness, corresponding to the development of ferromagnetism at around 4.5 ML. The ferromagnetic phase can be turned into a superparamagnetic phase by means of a thermal treatment. STM measurements allowed us to ascribe the onset of ferromagnetism to the transition from a three-dimensional to a two-dimensional growth mode of the iron deposit and to explain the superparamagnetic behavior in the annealed film as due to the formation of a collection of well-separated-squared iron particles. Moreover, using the particle shape and size distribution measured by STM, we calculated a value of the magnetic anisotropy of the Fe particles, which is 1 order of magnitude larger than the bulk iron one. This increase is mainly ascribed to the role of surface anisotropy in the Fe nanoparticles and also the role of the dipolar interactions between particles is discussed.

DOI: 10.1103/PhysRevB.79.035408 PACS number(s): 75.70.Cn, 75.30.Gw, 79.60.Jv, 68.55.−a

I. INTRODUCTION

The Fe/MgO(001) system is a model system for the investigation of the magnetic properties of iron nanostructures due to the good epitaxial relation between Fe and MgO (3.8% of lattice mismatch) and the weak interaction (from a magnetic and chemical point of view) between the substrate and the overlayer.[1,2] The possibility of obtaining almost isolated Fe nanostructures has driven a theoretical study[3] which has predicted a strong enhancement of the Fe magnetic moment for a monolayer of Fe deposited on MgO. This theoretical prediction has never been experimentally confirmed up to now and in the ultrathin limit of few Fe layers (<4 ML) many studies point to a superparamagnetic behavior of the iron films.[4–6] Increasing the Fe thickness, the superparamagnetic phase is replaced by a ferromagnetic phase at about 4 ML. The magnetic behavior of the iron films as a function of thickness is in general attributed to an initial three-dimensional (3D) growth and a successive coalescence of the iron islands into a continuous film, but recently a different model pointing to the role played by the substrate roughness has also been proposed.[4] Although the morphology of the Fe deposits is recognized to be a fundamental parameter in the determination of the magnetic properties of the Fe film, direct measurements by scanning probe microscopy (SPM) in the ultrathin limit (<10 ML) are scarce in the literature and only Fe films thicker than 5 nm have been well characterized.[7–9] In the literature the information on the morphology of the first stages of Fe growth of MgO is often inferred indirectly from the measurements of other properties, e.g., the magnetic behavior. It is in fact very hard to perform STM measurements on bulk MgO at low Fe coverages. The use of a MgO substrate in the form of a thin film (5 ML) grown on Ag(001) allowed us to overcome this difficulty. The choice of the silver substrate is motivated by the good crystalline quality of the MgO films grown on it[10,11] and by the fact that the presence of silver does not alter the magnetic properties of iron films. For these reasons we consider the Fe/MgO/Ag(001) as the ideal system for investigating the relationship between the morphology and the magnetic properties of iron thin films, in particular, in the first stages of the film growth (<10 ML).

In addition to this the study of the magnetic properties of iron in the Fe/MgO/Ag(001) has an applicative relevance due to the recent discovery of a large giant magnetoresistance (GMR) effect in Fe/MgO/Fe trilayers,[12] where the precise determination of the magnetic properties of Fe films on MgO films is mandatory for the optimization of magneto tunnel junction (MTJ) devices. Since the structure and morphology of a MgO film on Ag(001) are very similar to those of a MgO film on Fe(001),[13–15] the results of the present work can be of help also for the Fe/MgO/Fe system. Moreover, due to the tendency of microelectronics to move toward devices with nanometric lateral dimensions (thus approaching the superparamagnetic limits of the magnetic components) the study of the factors which influence the magnetic stability of Fe nanoparticles is also an interesting issue.

II. EXPERIMENT

The magnetic properties of Fe/MgO were studied by x-ray magnetic circular dichroism (XMCD) at APE beamline at the Elettra synchrotron radiation facility (Trieste, Italy).[16] The absorption spectra were recorded in total electron yield measuring the drain current. The light was circularly polarized with 75% of polarization degree and the beam was impinging at 45° with respect to the surface normal and was forming an angle of 45° with the direction of the magnetic field generated by a horseshoe magnet. The magnetic field was applied parallel to the [010] direction of iron. All

XMCD measurements were performed at remanence reversing the magnetization direction for each point of the spectra. The absorption spectra (relative to the parallel (p) and antiparallel (n) orientation of magnetization and light polarization) were divided by the incoming photon flux measured on a grid placed at the entrance of the experimental chamber. For all spectra, we have calculated the XMCD asymmetry defined as $[I(p)-I(n)]/[I(p)+I(n)]$. The obtained values have been successively corrected for the light polarization degree and geometrical factor. In order to exclude the presence of asymmetries in the magnetic field, we measured an XMCD spectrum using the two light polarizations after the application of a magnetic field of a few mT and compared it to the one measured after the application of the same magnetic field in the opposite direction. Since the measured spectra were identical, we excluded the presence of asymmetries or stray magnetic fields.

During the experiment we also recorded magnetic hysteresis loops of all the thickness analyzed. The hysteresis curves have been measured recording the absorption intensity of the L_3 edge and of a point at 695 eV of photon energy (just below the L_3 white line) as a function of the applied magnetic field. The L_3 signal has been divided by the pre-edge signal in order to remove the effect due to the presence of an applied magnetic field.

STM measurements were carried out at the SESAMO laboratory (Modena, Italy)[17] and their quantitative analysis has been performed using the WSXM program.[18]

In both experimental setups used in this work the samples were grown by molecular beam epitaxy (MBE) in a dedicated chamber and transferred in vacuum to the analysis chamber. The substrate used was a Ag(001) single crystal cleaned by repeated cycles of Ar^+ bombardment and annealing at 700 K. MgO films were prepared by evaporating Mg on the clean Ag surface in 5.3×10^{-8} hPa of oxygen pressure. During the growth of MgO the temperature of the substrate was kept at 460 K. The thickness of the MgO film was set to 5 ML for all the samples in this work. After the MgO growth we have verified the stoichiometry and thickness by x-ray photoemission spectroscopy (XPS) and Auger and the crystalline long-range order by low-energy electron diffraction (LEED). On this substrate we have evaporated Fe layers at room temperature. Partial shading of the sample during Fe evaporation resulted in a staircaselike iron film with 1 mm of step width with thickness ranging from 2 to 9 ML. In addition, in order to induce strong morphological changes, we have annealed a 4.5-ML-thick Fe sample at 673 K for 30 min and successively we have recorded the dichroic signal of the film at different temperatures ranging from 100 to 380 K. Moreover, one sample of 4.5 ML of thickness annealed at 673 K for 30 min was capped with 4 nm of Ag and 3 nm of MgO and then taken to air, where hysteresis cycles have been recorded by a magneto-optic Kerr effect (MOKE) apparatus. The MgO/Ag capping layer was chosen to be effective in preventing Fe oxidation after air exposure and to allow a MOKE signal to be measured from the Fe layer.

III. RESULTS AND DISCUSSION

A. As-deposited films

During the experiment we have recorded XMCD spectra of the as-grown iron deposits as functions of the film thickness. In Fig. 1 we show the absorption spectra of the $L_{2,3}$ edge of iron for the two different magnetization directions and the XMCD spectra of two significant samples, i.e., 3.3 and 7 ML Fe on 5 ML MgO/Ag(001). The absorption spectra have the typical smooth shape of the metallic character without localized states. For some chosen significant samples we have calculated the spin and orbital magnetic moments per atom (m_{spin} and m_{orb}) and their ratio with the sum-rules analysis.[19] The results are listed in Table I. Both m_{spin} and m_{orb}/m_{spin} resulted in agreement with the bulk iron values (2.1 and $0.045\mu_B$, respectively). It is important to underline that the m_{orb}/m_{spin} ratio does not present differences with respect to the normal bulk state because the m_{orb}/m_{spin} ratio is very sensitive to the modification of the electronic struc-

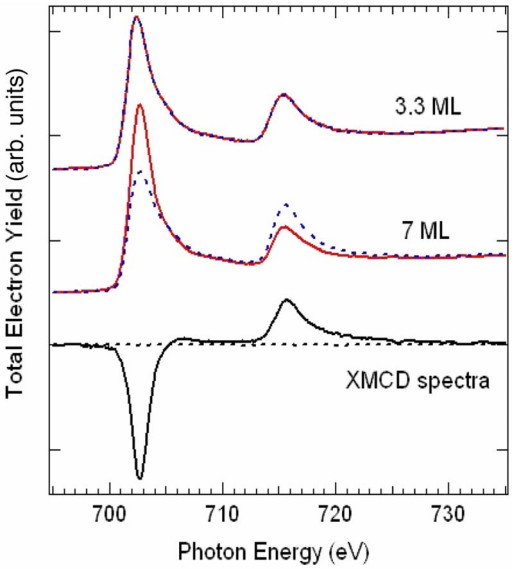

FIG. 1. (Color online) Top: Absorption spectra of the $L_{2,3}$ edges of iron of two iron films of 3.3 and 7 ML of thickness for the two different magnetization directions (continuous and dashed gray lines). Bottom: XMCD spectra of the 7 and 3.3 ML Fe films (continuous and dashed black line, respectively). The XMCD spectra have been corrected for the geometrical factor and light polarization degree.

TABLE I. Spin magnetic moment and orbital to spin magnetic-moment ratio for the different Fe thicknesses.

Thickness (ML)	M_{spin} (μ_B) $\pm0.1\mu_B$	M_{orb}/M_{spin} ±0.01
4	0	
4.2	0.4	0.04
4.5	1.1	0.05
4.9	1.7	0.04
5.2	2	0.05
6	2	0.04
7	2.1	0.04
8	2.1	0.04
8.9	2.2	0.04

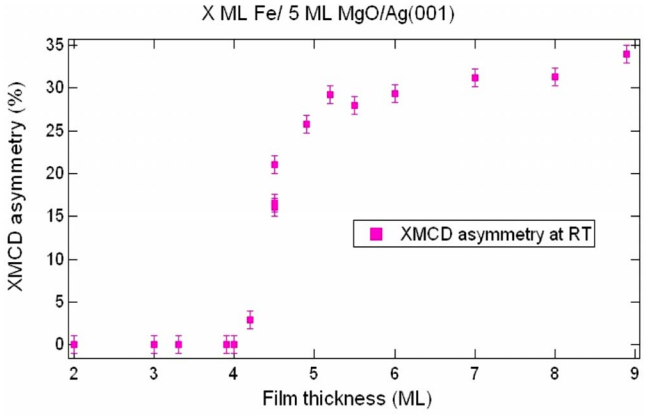

FIG. 2. (Color online) Value of the XMCD asymmetry at the maximum of the L_3 absorption edge plotted as a function of the Fe thickness.

ture connected to reduced dimensionality[20] or to the chemical environment.[21] Therefore from a spectroscopic point of view the electronic structure of the iron film is identical to the bulk iron one. This conclusion holds for all the samples presented in this work, i.e., no modifications of the electronic structure have been observed for different thicknesses or preparation procedures. These findings are not surprising considering that in a previous experiment on Fe/MgO (Ref. 22) we have observed deviations from the iron bulk L_3/L_2 branching ratio only below 2 ML and that in an XMCD experiment on preformed Fe clusters an increase in the orbital moment has been observed only for particles of 2.4 nm in diameter.[23]

In Fig. 2 we show the XMCD asymmetry as a function of Fe thickness at room temperature. Below 4.5 ML the samples gave a zero net magnetic response. The dichroic signal appears at about 4.5 ML Fe thickness and it rapidly increases, becoming constant for thicknesses larger than 5.5 ML. Thus the transition to the ferromagnetic phase is delimited in a narrow region of about 1 ML. The variations in XMCD amplitude can, in general, be ascribed either to changes in the local magnetic moment or to variations in the magnetic long-range order within the analyzed area. Since, as previously stated, the XMCD spectra show that the local magnetic moment is constant for all the Fe thicknesses analyzed in this work, the observed variation in the XMCD signal with Fe thickness is due to changes in the magnetization at remanence.

Together with the XMCD spectra we have recorded hysteresis loops for all the thicknesses analyzed. In Fig. 3(a), the loops corresponding to the different thickness of the wedged sample are presented. The hysteresis curves are squared and only those corresponding to the transition region are slightly elongated. The coercive field is of a few tenths of mT for the deposits of about 5 ML and steadily increases as a function of iron thickness reaching 2 mT for a 9 ML film.

The morphology of the iron film was investigated by STM. In Fig. 4 we present the images corresponding to Fe deposits of 3.5, 6.5, and 7.5 ML on 5 ML MgO/Ag(001). For all thicknesses the surface is uniformly covered by small 3D Fe clusters. The cluster height does not change significantly

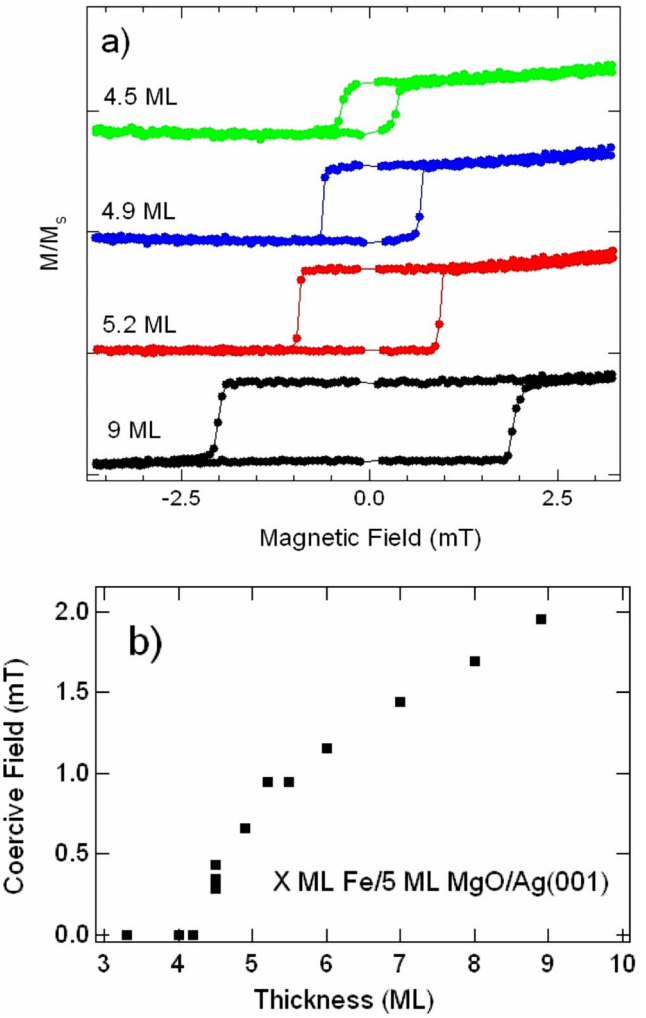

FIG. 3. (Color online) (a) Hysteresis curves measured at room temperature for different Fe deposits. (b) Value of the coercive field plotted as a function of the Fe thickness.

as a function of the film thickness, ranging from 0.2 to 2 nm with an average value of approximately 1.2 nm, as shown by the height profiles in Fig. 4. The overestimation of the cluster height can be understood taking into account that the STM measurement is influenced by the electronic structure of the probed surface and therefore the presence of uncovered MgO can severely affect the measured cluster height.[24] The lateral dimensions of the clusters show a clear evolution with the thickness of the Fe film: in the thinnest film the average cluster area is 25 nm^2 while in the 6.5 and 7.5 ML samples it is 37 nm^2. From the STM images it is not possible to directly determine a critical thickness for coalescence; but, considering that from 3.5 to 6.5 ML the clusters' lateral size is markedly increased while from 6.5 to 7.5 ML the morphology is not significantly changed, it is reasonable to assume that between 3.5 and 6.5 ML of thickness the iron growth mode undergoes a transition from a 3D Volmer-Weber growth mode to a two-dimensional (2D) growth mode.

In summary, the behavior of the magnetization as a function of the iron film thickness shows a quite sharp transition to the ferromagnetic regime at 4.5 ML rapidly saturating to a full magnetization condition for films thicker than 5 ML,

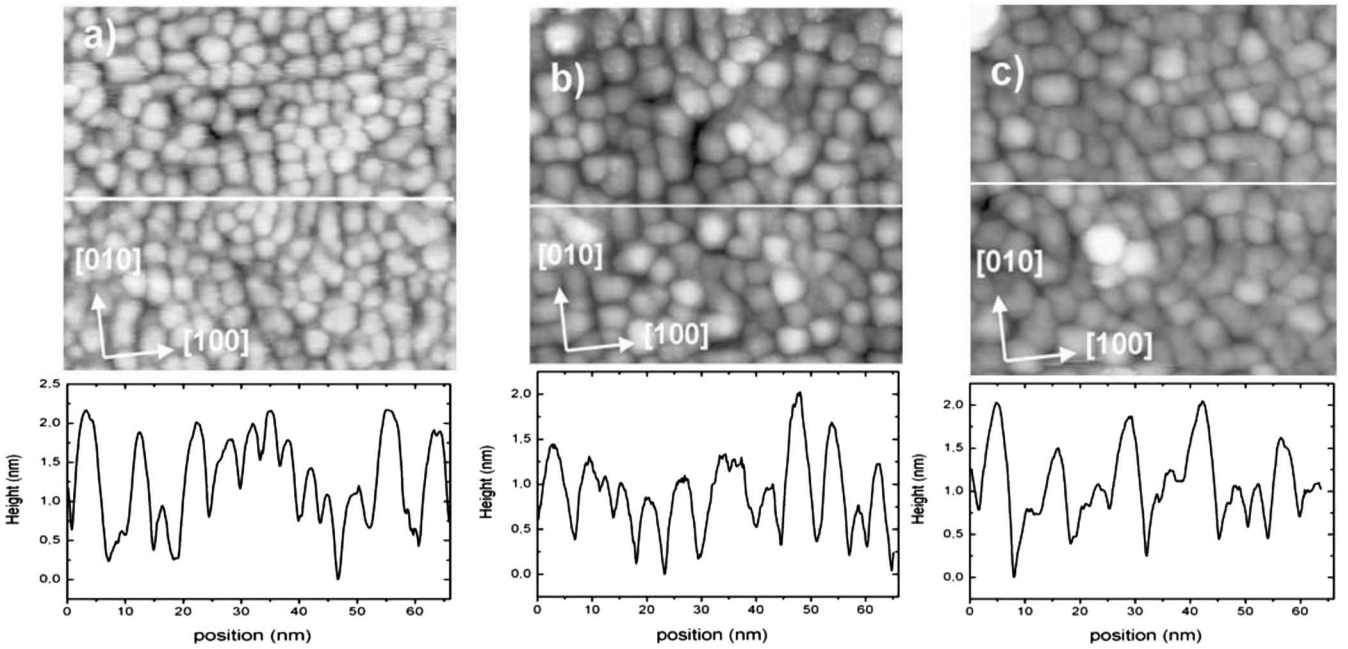

FIG. 4. 65×65 nm^2 STM image (1.8 V, 0.1 nA) of (a) 3.5, (b) 6.5, and (c) 7.5 ML Fe on 5 ML MgO/Ag(001). Bottom: Height profiles of the STM images along the horizontal lines indicated in the images.

while the thinner deposits (<4 ML) do not show any magnetic remanence. This observation is in agreement with previous results[4–6] on Fe film grown on MgO(001) single crystals. In these works the authors ascribe the absence of magnetic signal in the ultrathin limit to a superparamagnetic phase of iron due to discontinuous Fe films. However, in these works the information on the morphology of Fe at low coverages indirectly inferred from the magnetic measurements by calling into play either a 3D growth[5,6] or the presence of MgO steps avoiding the formation of large Fe terraces.[4] In this work the STM images clearly demonstrate that the initial Fe growth is in the 3D Volmer-Weber mode and as a consequence the small volume of the Fe clusters determines a superparamagnetic phase which gives zero net magnetization at room temperature. In fact a film of 3.5 ML of thickness shows clusters of 25 nm^2 of base and consequently each cluster is formed by only 1000 atoms. Also the transition to the ferromagnetic phase finds its origin in the morphology of the iron film. In fact we have observed that the growth mode changes to a 2D mode between 3.5 and 6.5 ML, thus determining the coalescence of the clusters in large agglomerates, which assume the volume needed for the onset of ferromagnetism.

The coercivity of the iron film displays an almost linear behavior as a function of the thickness, starting from 0.4 mT at 5 ML (where the magnetization is already saturated) the coercivity steadily increases up to a value of 2 mT for a 9 ML thick film [Fig. 3(b)]. It is interesting to compare this result with the values of coercivity obtained for thicker Fe films in previous works in which values of about 1 mT of coercivity for a 5-nm-thick film (35 ML) (Ref. 7) and 0.8 mT for 3.58 nm film[9] were reported. These numbers do not follow the linear trend we observe in the first nine layers and indicate the existence of a critical thickness above which the coercivity decreases. A similar behavior has been previously observed in thin Co films deposited onto the Cu(001) surface where the coercivity increases linearly between 2 and 7 ML and then slowly decreases.[25] The authors attribute the coercivity variation as a function of thickness to the thickness dependence of the Néel walls energy. At variance with the Co/Cu(001) case we have not observed saturation up to 9 ML and, if we consider the coercive fields measured in previous works,[7,9] the decrease in coercive field above the critical thickness would be more pronounced. The study of this effect, which goes beyond the scope of the present work, would be interesting both to understand the complex micromagnetic mechanism responsible for it and in view of a possible application in magnetoresistive and magnetotunnel multilayers, suggesting the possibility to produce magnetic layers with different switching fields by simply alternating layers of different thickness.

B. Annealed sample

During the experiment we have annealed a deposit of 4.5 ML of thickness at 673 K for 30 min and we have investigated the effect of the thermal treatment on the magnetic properties of the Fe layer. It turns out that the magnetism of the annealed sample is dramatically changed with respect to the as grown sample; in fact the XMCD asymmetry dropped from 21% to 10% after the annealing procedure.

This sample did not show a hysteresis loop in the magnetic field range used for the room-temperature deposited samples. However, when we tried to measure the loops using a larger magnetic field range, we observed the appearance of a high background, probably due to the influence of magnetic field on the secondary electrons. This effect hindered the possibility to acquire a complete loop on the annealed sample. On this sample we measured a nonzero remanent XMCD signal only after the application of a magnetic field

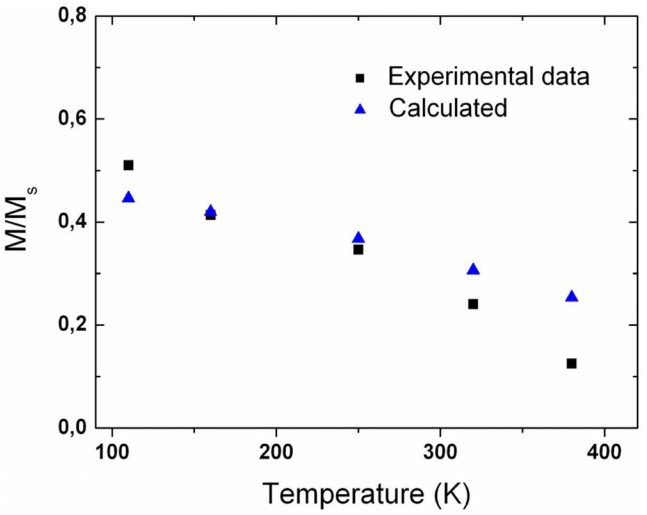

FIG. 5. (Color online) Experimental (triangles) and calculated (squares) remanence to saturation magnetization ratio as a function of temperature for a 4.5-ML Fe-thick deposit annealed at 673 K for 30 min. The size of the points (±0.015 on the vertical axis) accounts for the experimental error.

of 40 mT. This represents a further difference in the magnetic behavior of the sample after the annealing process. The room-temperature deposited sample in fact showed a remanent magnetization after the application of much lower magnetic fields and the remanence and saturation magnetization coincide above approximately 0.8 mT. As discussed in the following, this behavior can be explained taking into account the differences in morphology.

On the annealed sample, we have performed a temperature dependence study of the magnetic signal from 100 to 380 K by cooling the sample in zero field and then performing XMCD measurement raising the temperature by steps. In Fig. 5 the behavior of the ratio of remanence to saturation magnetization as a function of temperature is shown. The ratio increases monotonically decreasing the temperature from 12% at 380 K to 51% at 100 K.

Also from a morphological point of view the annealing determines drastic changes. Figure 6 shows the STM image of the 4.5 ML Fe or 5 ML MgO/Ag(001) sample after the thermal treatment. The light gray squared or rectangular

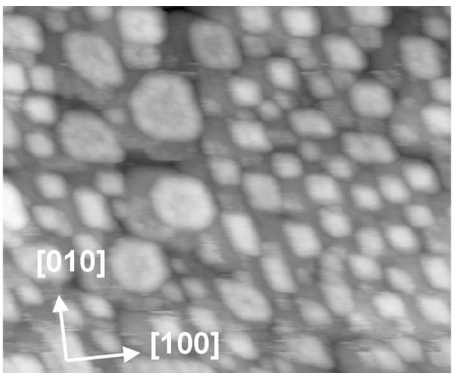

FIG. 6. 80×60 nm^2 STM images (2.0 V, 0.1 nA) of 4.5 ML Fe on 5 ML MgO/Ag(001) annealed at 673 K for 30 min.

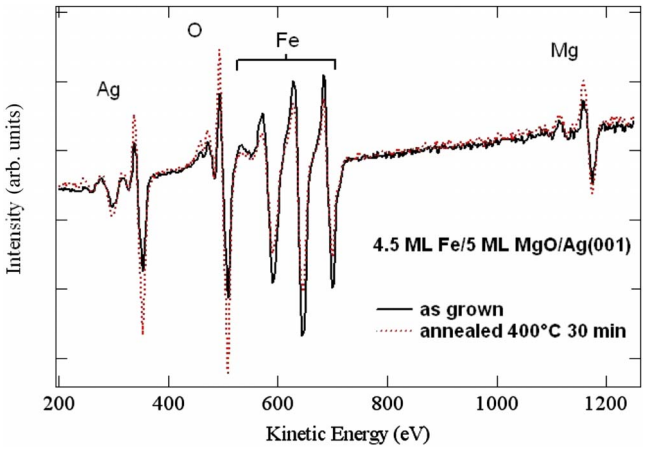

FIG. 7. (Color online) Auger spectra before (black continuous line) and after (gray dotted line) the annealing process of the 4.5 ML Fe deposit. The spectra were measured using 3 keV of primary beam energy.

clusters have been ascribed to Fe, while the gray background has been ascribed to the MgO film with terraces (gray areas) and small holes (dark gray areas). The size distribution of the Fe clusters is quite broad: the larger clusters occupy an area of 150 nm^2 while the smallest occupies only 20 nm^2. Unlike the size distribution, the height distribution is very narrow around a mean value of 2 nm. The large majority of the cluster edges are aligned along the ⟨100⟩ direction of iron. The total fraction of the surface covered by these clusters results to be approximately 45%, as measured on the STM images. To unambiguously assign these clusters as iron clusters, we have recorded Auger spectra (Fig. 7) before and after the annealing process. The thermal treatment induces a severe decrease in the ratio between the intensity of the Fe Auger lines and the intensity of the Mg and O Auger lines. Under the hypothesis of a starting continuous film of 0.64 nm of thickness that aggregates into thicker clusters leaving uncovered parts of the surface and assuming a 1.2 nm of electron attenuation length (EAL) for the Fe line and a 1.1 nm EAL for the O line,[26] we have calculated that the Auger spectrum corresponds to a surface covered by Fe clusters 1.5 nm thick with a fractional coverage of 43% of the MgO surface. Thus the Auger spectroscopic measurements are in very good agreement with the topographic observations and confirm the assignment of the light gray islands as Fe clusters.

Previous works on thicker Fe films deposited on MgO(001) single crystal report that the growth of Fe at elevated temperature or post-annealing treatments determine a morphological configuration with disconnected Fe islands[27] which display a superparamagnetic behavior.[7,9,28] We observe the same effect but, in the present case, the Fe deposit was thinner compared to previous works, and therefore the agglomeration process due to thermal treatment gives rise to a collection of Fe particles well separated from each other. As evidenced from the magnetization temperature dependence, this collection of iron nanoparticles is in a superparamagnetic phase.

In the superparamagnetic theory, the magnetic moment of a particle continuously attempts to flip from one direction to

another with a given periodicity (t_0) which is characteristic for each system [in iron it is about 10^{-12} s (Ref. 4)] due to thermal fluctuations. The energy barrier that has to be overcome to effectively flip between two different directions depends on the term $K_{\text{eff}}V$ (where K_{eff} is the effective magnetic anisotropy and V is the volume of the magnetic particle). Thus, according to the superparamagnetic theory, a particle that has been oriented by an external magnetic field has a finite probability to have the same orientation after the measurement time (t) and this probability is given by the formula

$$\rho(T,V,t) = e^{-t/\tau} \quad \text{where} \quad \tau = t_0 e^{K_{\text{eff}}V/K_B T}.$$

According to this formula the probability increases if the temperature is lowered until the particle reaches its "blocking temperature" and consequently a freezing of the spin direction occurs. This mechanism determines the shape of the zero-field-cooled (ZFC) magnetization temperature dependence in superparamagnetic systems.[29] The description of the magnetization behavior of a collection of particles as a function of temperature (or time) in the framework of the superparamagnetic theory is complicated by the unavoidable size distribution of the particles which is not always known with precision. In the present study, thanks to the STM measurement, we know the particle size distribution with precision and therefore we can solve numerically the integral that describes the magnetization M at different temperatures,

$$M(T,t) \propto \int \rho(T,t,V) f(V) V dV,$$

where $f(V)$ is the volume size distribution of the iron particles. This description neglects the reduction in the measured magnetization due to the blocked particles in the low-temperature region; but in our data the peak of the ZFC curves is not visible and consequently we consider that only the point at the lowest temperature can be slightly affected by this reduction. The calculated magnetization vs temperature dependence (Fig. 5) is in qualitative agreement with our experimental result if a value of 4.6×10^5 J m^{-3} for the K_{eff} term is used. This value for the magnetic anisotropy is 1 order of magnitude larger than the one of bulk iron. Significant increases in the magnetic anisotropy in iron nanoparticles have been already observed[30–32] and, in particular, Park *et al.*[28] studied the same system adopting a similar sample preparation procedure and estimated the K_{eff} of a 10 ML Fe deposit to be between 5.2 and 6.7×10^5 J m^{-3}. At variance with the study of Park *et al.* in the present case, we have not observed the typical peak of the ZFC curve down to 100 K. This difference is attributable to the smaller mean size of the Fe clusters in the present work due to the smaller thickness of the Fe deposit in our case. It is not trivial to ascribe the observed increase in the magnetic anisotropy to a precise effect because the K_{eff} term includes all the energetic terms of the system (cubic, surface, interface, shape anisotropies and also the particle-particle interactions). Nonetheless, the previous studies all point to the increased weight in the surface anisotropy. To evaluate the impact on the magnetic anisotropy of the increased surface to bulk ratio in our iron nanoparticles, we can use the formula $K_{\text{eff}}V = K_s S + K_v V$ (where K_s and K_v are the iron surface and bulk anisotropy, respectively). Taking into account the particle size distribution measured by STM and assuming 4.6×10^4 J m^{-3} for the bulk iron and 1.0×10^{-3} J m^{-2} for the iron surface anisotropy,[33] we have calculated the average K_{eff} of our system that results to $K_{\text{eff}} = 3.1\times10^5$ Jm^{-3} very close to the observed value of 4.6×10^5 J m^{-3}. In this calculation we have taken into account only the lateral surfaces of the iron particle because due to the experimental geometry we measure only the in-plane component of the magnetization, and therefore the upper surface which tends to align the magnetization perpendicularly to the surface does not contribute to the measured anisotropy. The good agreement between the estimated and the measured values of the magnetic anisotropy of the Fe nanoparticles shows that even if probably it is not the sole parameter, the surface anisotropy plays a major role in the measured enhancement. Nonetheless, due to the high density of magnetic particles on our sample the role of the interparticle interactions must also be considered. The effects of such interaction have been investigated both in magnetic particles dispersed in liquid solutions[34–36] and self-assembled on flat surfaces.[37,38] In a schematic way a collection of superparamagnetic particles can be classified as a noninteracting, weakly interacting, or strongly interacting system. In the first case the system behaves like a collection of isolated superparamagnetic particles; in the weakly interacting systems the dipole-dipole interaction modifies the dynamical properties but it is still possible to describe the magnetic behavior of the system in the framework of the superparamagnetic theory by increasing the energy barrier (increasing the K_{eff} term) accounting for the interparticle interaction; while in the strongly interacting systems magnetic phase transitions occur and the collective modes are no longer described by the superparamagnetic theory.

A simple way to evaluate the impact of the particle-particle interaction on the magnetic properties of the system starting from the analysis of the hysteresis cycles was proposed by Allia *et al.*[39] In this model an apparent temperature is introduced in the argument of a Langevin function that describes the behavior of a pure superparamagnetic system, in order to account for the contribution coming for the interparticle interactions. To investigate this point we have prepared the same sample used for XMCD measurements, capped it with 4 nm of Ag and 3 nm of MgO, and we have recorded hysteresis loops, *ex situ* at room temperature, with a MOKE apparatus. We have averaged the two branches of the cycles and compared the result with a sum of 30 Langevin functions with different magnetic moments weighted according to the size distribution obtained from STM measurements. The result is shown in Fig. 8, where the open points are the experimental data and the continuous line is the simulated cycle. The good agreement between the experimental and calculated curve is remarkable, since the calculated curve is not the result of a fit procedure but merely the application of the superparamagnetic theory with all parameters (magnetic field, magnetic-moment distribution, and temperature) coming from the experimental measurements. The small difference between the calculated and the measured M vs H curve becomes negligible by modifying the temperature in the argument of the Langevin function by only 40 K,

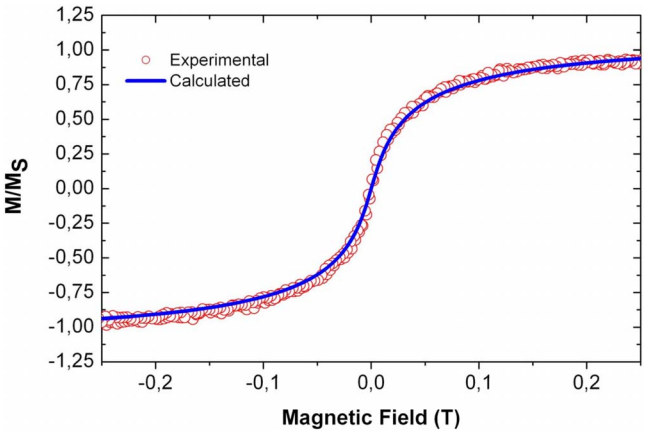

FIG. 8. (Color online) M/M_s vs H curve of 3 nm MgO/4 nm Ag/4.5 ML of Fe/10 ML MgO/Ag(001) annealed sample measured with MOKE apparatus at room temperature (open red circles). Superposition of a set of 30 Langevin functions with different magnetic moments weighted for the cluster size distribution obtained from STM measurements (continuous blue line).

indicating a very weak interparticle interaction. Moreover, this difference is within the error bar of our measurement given the unavoidable uncertainties in the determination of the film thickness and cluster size distribution. This measurement thus demonstrates that the dipolar interactions have little impact on the magnetic properties of the system, which can be fairly described in the framework of the superparamagnetic theory.

IV. CONCLUSIONS

In this study we have coupled STM and XMCD measurements to investigate the relationship between the morphological arrangement and the magnetic properties of the Fe/MgO system. We give clear experimental evidence that Fe grows on the MgO substrate in a 3D mode and only at about 4.5 ML of thickness the clusters coalesce. Associated to this coalescence we observe the onset of ferromagnetism. Moreover, we have shown that the magnetic properties of Fe film, continue to evolve as a function of thickness also beyond the stabilization of the ferromagnetic phase increasing the coercivity linearly with thickness for several layers. This effect needs to be further investigated because it can have possible application in magnetoresistive devices by simplifying the complex multilayers architecture. Once the ferromagnetic phase is reached (i.e., for deposit of >4.5 ML), it is possible to obtain a superparamagnetic phase with a thermal treatment of the sample. In fact, postannealing causes the agglomeration of the Fe deposit in squared or rectangular clusters forming a collection of disconnected Fe nanoparticles which shows a superparamagnetic behavior. These clusters have a magnetic anisotropy that is 1 order of magnitude larger than the Fe bulk one, mainly originating from the enhanced role of the surface anisotropy in the Fe nanoparticles.

ACKNOWLEDGMENTS

This work has been supported by E.U. within the project FP6STRP "GSOMEN" under Contract No. NMP4-CT-2004-001594.

[1] P. Luches, S. Benedetti, M. Liberati, F. Boscherini, I. I. Pronin, and S. Valeri, Surf. Sci. **583**, 191 (2005).
[2] M. Sicot, S. Andrieu, F. Bertran, and F. Fortuna, Phys. Rev. B **72**, 144414 (2005).
[3] Chun Li and A. J. Freeman, Phys. Rev. B **43**, 780 (1991).
[4] C. Martínez Boubeta, C. Clavero, J. M. García-Martín, G. Armelles, and A. Cebollada, Ll. Balcells, J. L. Menéndez, F. Peiró, A. Cornet, and M. F. Toney, Phys. Rev. B **71**, 014407 (2005).
[5] C. Liu, Y. Park, and S. D. Bader, J. Magn. Magn. Mater. **111**, L225 (1992).
[6] S. Adenwalla, Y. Park, G. P. Felcher, and M. Teitelman, J. Appl. Phys. **76**, 6443 (1994).
[7] S. M. Jordan, J. F. Lawler, R. Schad, and H. van Kempen, J. Appl. Phys. **84**, 1499 (1998).
[8] S. M. Jordan, R. Schad, A. M. Keen, M. Bischoff, D. S. Schmool, and H. van Kempen, Phys. Rev. B **59**, 7350 (1999).
[9] A. Subagyo, K. Sueoka, K. Musaka, and K. Hayakawa, Jpn. J. Appl. Phys., Part 1 **38**, 3820 (1999).
[10] S. Valeri, S. Altieri, U. del Pennino, A. di Bona, P. Luches, and A. Rota, Phys. Rev. B **65**, 245410 (2002).
[11] S. Altieri, S. Valeri, A. di Bona, P. Luches, C. Giovanardi, and T. S. Moia, Surf. Sci. **311**, 507 (2002).
[12] S. Yuasa, T. Nagahame, A. Fukushima, Y. Suzuki, and K. Ando, Nat. Mater. **3**, 868 (2004).
[13] J. Wollschlager, D. Erdos, H. Goldbach, R. Hopken, and K. M. Schroder, Thin Solid Films **400**, 1 (2001).
[14] J. L. Vassent, M. Dynna, A. Marty, B. Gilles, and G. Patrat, J. Appl. Phys. **80**, 5727 (1996).
[15] M. Klaua, D. Ullmann, J. Barthel, W. Wulfhekel, J. Kirschner, R. Urban, T. L. Monchesky, A. Enders, J. F. Cochran, and B. Heinrich, Phys. Rev. B **64**, 134411 (2001).
[16] http://www.tasc.infm.it/research/ape/scheda.php
[17] http://www.sesamo.unimo.it/
[18] I. Horcas, R. Fernández, J. M. Gómez-Rodríguez, J. Colchero, J. Gómez-Herrero, and A. M. Baro, Rev. Sci. Instrum. **78**, 013705 (2007).
[19] C. T. Chen, Y. U. Idzerda, H. J. Lin, N. V. Smith, G. Meigs, E. Chaban, G. H. Ho, E. Pellegrin, and F. Sette, Phys. Rev. Lett. **75**, 152 (1995).
[20] P. Gambardella, A. Dallmeyer, K. Maiti, M. C. Malagoli, W. Eberhardt, K. Kern, and C. Carbone, Nature (London) **416**, 301 (2002).
[21] P. Torelli, F. Sirotti, and P. Ballone, Phys. Rev. B **68**, 205413 (2003).
[22] P. Luches, P. Torelli, S. Benedetti, E. Ferramola, R. Gotter, and S. Valeri, Surf. Sci. **601**, 3902 (2007).
[23] K. W. Edmonds, C. Binns, S. H. Baker, S. C. Thornton, C. Norris, J. B. Goedkoop, M. Finazzi, and N. B. Brookes, Phys. Rev. B **60**, 472 (1999).

[24] R. Shantyr, Ch. Hagendorf, and H. Neddermeyer, Thin Solid Films **464–465**, 65 (2004).
[25] Q. Jiang, H.-N. Yang, and G.-C. Wang, Surf. Sci. **373**, 181 (1997).
[26] C. J. Powell and A. Jablonski, *NIST Electron Effective Attenuation Length database, Version 1.0* (National Institute for Standard and Technology, Gaithersburg, MD, 2001).
[27] A. di Bona, C. Giovanardi, and S. Valeri, Surf. Sci. **498**, 193 (2002).
[28] Y. Park, S. Adenwalla, G. P. Felcher, and S. D. Bader, Phys. Rev. B **52**, 12779 (1995).
[29] R. Sappey, E. Vincent, N. Hadacek, F. Chaput, J. P. Boilot, and D. Zins, Phys. Rev. B **56**, 14551 (1997).
[30] D. L. Peng, T. Hihara, K. Sumiyama, and H. Morikawa, J. Appl. Phys. **92**, 3075 (2002).
[31] F. Bødker, S. Mørup, and S. Linderoth, Phys. Rev. Lett. **72**, 282 (1994).
[32] C. Binns, M. J. Maher, Q. A. Pankhurst, D. Kechrakos, and K. N. Trohidou, Phys. Rev. B **66**, 184413 (2002).
[33] K. B. Urquhart, B. Heinrich, J. F. Cochran, A. S. Arrott, and K. Myrtle, J. Appl. Phys. **64**, 5334 (1988).
[34] J. L. Dormann, L. Bessais, and D. Fiorani, J. Phys. C **21**, 2015 (1988).
[35] S. Mørup and E. Tronc, Phys. Rev. Lett. **72**, 3278 (1994).
[36] D. Fiorani, J. L. Dormann, R. Cherkaoui, E. Tronc, F. Lucari, F. D'Orazio, L. Spinu, M. Nogues, A. Garcia, and A. M. Testa, J. Magn. Magn. Mater. **196-197**, 143 (1999).
[37] P. Poulopoulos, P. J. Jensen, A. Ney, J. Lindner, and K. Baberschke, Phys. Rev. B **65**, 064431 (2002).
[38] M. R. Scheinfein, K. E. Schmidt, K. R. Heim, and G. G. Hembree, Phys. Rev. Lett. **76**, 1541 (1996).
[39] P. Allia, M. Coisson, P. Tiberto, F. Vinai, M. Knobel, M. A. Novak, and W. C. Nunes, Phys. Rev. B **64**, 144420 (2001).